J. Materials, Conc. Struct., Pavements No. 520/V-28, 297-308, August 1995

EFFECTIVENESS OF LATERALLY ARRANGED REINFORCEMENT ON THE CONFINEMENT OF CORE CONCRETE

Tirath Manojya PALLEWATTA[1], Paulus IRAWAN[2] and Koichi MAEKAWA[3]

[1] Dr. of Eng., Former Graduate Student, Dept. of Civil Eng., The University of Tokyo (Hongo 7-3-1, Bunkyo-ku, Tokyo 113, Japan)
[2] Member of JSCE, Ms. of Eng., Graduate Student, Dept. of Civil Eng., The University of Tokyo (Hongo 7-3-1, Bunkyo-ku, Tokyo 113, Japan)
[3] Member of JSCE, Dr. of Eng., Associate Prof., Dept. of Civil Eng., The University of Tokyo (Hongo 7-3-1, Bunkyo-ku, Tokyo 113, Japan)

Behavior of concrete confined by lateral reinforcement is addressed through experimental approach. The primary objectives of the experimental study are to mechanically define the confinement effectiveness of lateral reinforcement layouts and to obtain reliable data for verification of non-linear, three dimensional concrete constitutive law under non-uniform stress field produced in confined concrete cores of column members. Further, identification of the influence of detailing parameters on the confinement phenomena was aimed for the purpose of developing and examining a behavior oriented macro-model.

Key Words *: confinement, lateral reinforcement, strength, ductility*

1. INTRODUCTION

Under passive lateral confinement provided by lateral steel, enhancement in the axial performance of concrete has been addressed owing to its beneficial effects on ductility and capacity of members, and design formulas (macro models) have been proposed for peak items of confined concrete[2),12)]. It can be seen that these are not directly associated with microscopic aspects of confinement, but rather developed through empirical approaches to represent experimental facts of interest in practice.

As a recent development, 3-dimensional constitutive models at a local point of confined concrete and computational tools enable stresses, plasticity and damage fields arising in a real member to be computed with less effort[4),5)]. These simulations can in turn be used to check the validity of microscopic models of concrete, too. In fact, for getting universal computational tools, experimental verification is most crucial at the member level where non-uniform stress field is produced[8)]. It may be agreed that data on capacity of confined concrete columns are so much available, but very few articles which are useful for experimental verification of microscopic constitutive models.

To fill this gap, verification oriented idealized experiments were conducted in the following four points; 1) no concrete cover to avoid non-confined zone of concrete, 2) closed loop welded ties designed for perfect anchorage of lateral reinforcement, 3) round bars used to eliminate bond and to measure strains in a whole zone and 4) no longitudinal bar to avoid load carrying mechanism by steel and to concentrate authors' discussion on compressive concrete under 3-D stresses. The engineering point of importance is to experimentally identify induced "real confining stresses" which is related to strength enhancement of core concrete and a target of verification of micro-models. As stated above, the main aim of this study is to obtain reliable data for verification of 3D constitutive laws of concrete[7)] on member level through computational approach.

The stress-strain behavior of concrete comprises of both non-linear ascending and descending branches. In the strain softening part, the compressive strain measurement is much affected by the loading rate and specimen size due to strain localization. Since the major objective of this study is to get the systematically arranged data available for verification of constitutive law of concrete, the ascending branch which portrays the pre-peak behavior and can be obtained with higher precision is firstly focused.

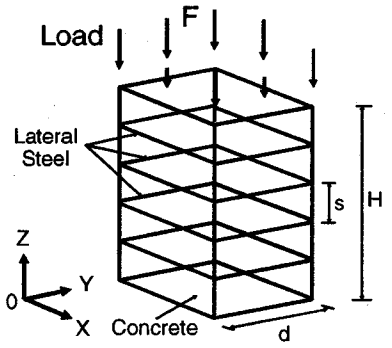

Fig.1 Confined concrete core

2. CONFINEMENT EFFECTIVENESS INDEX

Three-dimensional stresses in core concrete are non-uniform except for cylindrical cores confined by hydraulic pressure or by a steel cylinder. Then, indexes to represent confinement effectiveness of 3D-arranged lateral ties under non-uniform fields of stresses are needed and have to be experimentally identified, too. The authors introduced three indexes defined at a local point, a section and an entire volume of a concrete member, respectively[4),5)].

Reference system is taken such that x and y axes are in lateral orthogonal directions while z axis is along the axis of the confined core as shown in **Fig. 1.** The lateral confining stress at a point (x,y,z) is defined as in-plane first invariant (Eq.(1)) of lateral stress. By integrating this over the domain of (x-y) cross-section, *sectional average confining stress* denoted by $\overline{\sigma}_c$, is obtained as,

$$\sigma_c \equiv \frac{\sigma_{c,xx}+\sigma_{c,yy}}{2} \tag{1}$$

$$\overline{\sigma}_c = \overline{\sigma}_c(z) = \frac{1}{A_c}\int_{A_c} \sigma_c(x,y,z)\, dx\, dy \tag{2}$$

where, A_c is the domain of the cross section and $\sigma_{c,ij}$ is concrete stress tensor.

Further integration of the sectional average confinement along the axis of the core results in *spatial average confining stress* denoted by σ_v, which is the volumetric average of the lateral confining stresses induced to concrete as,

$$\sigma_v \equiv \frac{1}{H}\int_H \overline{\sigma}_c\, dz = \frac{1}{V_c}\int_{Vc} \frac{\sigma_{c,xx}+\sigma_{c,yy}}{2} dV \tag{3}$$

where, V_c is the volume domain of the core while H is length in z-direction of the core enclosed by hoops.

By applying the virtual work principle, equilibrium condition existing between confining steel and confined core can be proven[4)] as Eq.(4) where σ_s and V_s are steel fiber stress along axes of lateral reinforcing bars and steel volume, respectively.

$$\sigma_v = -\frac{1}{2V_c}\int_{V_s} \sigma_s dV \tag{4}$$

This relation in Eq.(4) is of great importance since averaged confining stress is equated to the spatially averaged steel stress integrated over its domain. Peak of this quantity which reflects the maximum level of confinement that can be generated will be attained when all provided steel comes to yield. Generation of this limit condition is depicted through Eq.(5) where, p is the volumetric lateral reinforcement ratio and f_y is the yield strength of steel.

$$\sigma_{v,\lim} = -\frac{1}{2}\left(\frac{V_s}{V_c}\right) f_y = -\frac{1}{2} p \cdot f_y \tag{5}$$

Ratio between actual confinement denoted by Eq.(4) and the maximum attainable in Eq.(5) is utilized to indicate the mechanically defined confinement effectiveness of a particular detailing as given in Eq.(6), which will be referred to as *confinement effectiveness index* newly introduced to quantify the confinement effectiveness on a theoretical basis. Also, the possibility of experimentally obtaining this index would serve to verify numerical modeling of materials as well as structures.

$$\alpha = \sigma_v / \sigma_{v,\lim} \tag{6}$$

Through the above discussions it is clear that if 3-D axial stress distribution of the confining steel in the whole domain can be obtained, spatial average confining stress applied to concrete can be computed. In order to get the axial stress distribution of the confining steel, strain measurements at discrete locations along a tie on two extreme fibers at each location has to be carried out. With the information of stress-strain relation of steel and "*plane section hypothesis*", the stress distribution across the cross section of the ties can be computed. Through such discrete measurements along tie arms, average confining stress of 3D can be experimentally computed by Eq.(4).

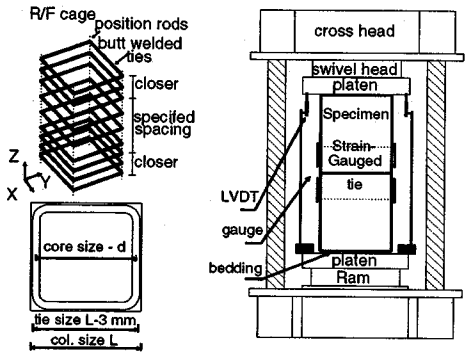

Fig.2 Specifications and experimental setup

3. EXPERIMENTAL APPROACH

(1) Specifications

Square discretely lateral reinforced concrete columns without longitudinal reinforcement nor cover concrete for lateral ties were selected for simple and clear boundary conditions which are beneficial for experimental verification of computational models as stated in Chapter 1. Along with reinforced specimens, plain concrete columns of the same dimension were cast to get the unconfined capacity for comparison.

The grade of steel used for all experiments was the same with yield strength in a close range for different bar diameters. Confined concrete core is herein defined as the one bound by centerlines of peripheral ties as shown in **Fig.2.** The experimental series are categorized in line with 1) the size effect of core with the same reinforcement ratio ($p \approx 4.5\%$), and the same spacing ratio ($s/d \approx 0.3$: See **Fig.1**.), 2) the effect of lateral reinforcement ratio and spacing with the same grade of steel and 3) the effect of flexural stiffness of tie arms by removing contact of core concrete with the tie arms except at corners. In this series of tests, higher reinforcement ratio cases compared with practically constructed columns are included in order to get data of wide variety for verifying constitutive model of concrete as stated in Chapter 1. Detailing parameters are summarized in **Table 1**.

(2) Fabrication

Lateral reinforcement used is square and formed by plain round bar as shown in **Fig.2**. In reality, the anchorage condition of both ends of a bent bar to form a tie would determine the performance of lateral confinement significantly. Since uncertain boundary conditions would result in unfeasible data for verifying computational models, it was decided to form lateral ties closed by complete welding. Butt welding was carried out by chamfering the facing edges with a filler metal to bridge the gap resulting in a continuous tie section instead of an enlarged lap at the weld.

Table 1 Detailing for experiments

Designation and Comments	Col. Size (L) (mm)	Tie Dia. (Ø) (mm)	Core Size (d) (mm)	Tie Spac. (s) (mm)	r/f ratio (p) (%)	Spac ratio (s/d)
C16-075, High r/f	200	15.70	181.3	75	5.70	0.41
D19-104, High r/f	200	18.70	178.3	104	5.92	0.58
O19x2-232, High r/f	200	18.80	178.2	232	5.37	1.20
A09-042, Medium r/f	200	9.00	188.0	42	3.22	0.22
H133-094, Medium r/f	200	12.95	184.1	94	3.05	0.51
I16-150, Medium r/f	200	15.85	181.2	150	2.91	0.83
J19-225, Medium r/f	200	18.80	178.2	225	2.77	1.26
M09-090, Low r/f	200	9.00	188.0	90	1.50	0.48
N13-192, Low r/f	200	12.95	184.1	192	1.49	1.04
P09-043, Size Effect Small Core	150	9.00	139.0	43	4.26	0.31
S25-119, Size Effect Big Core	400	24.80	373.2	119	4.35	0.32
T13-065, Size Effect Flex. Effect	200	12.95	184.1	65	4.40	0.35
U13-065-C, Corner Action, Flex. Effect	200	12.95	184.1	65	4.40	0.35
V16-075-LS, High r/f Low conc. strength	200	15.85	181.2	75	5.81	0.41

Ties were fabricated to very close tolerances, in order to achieve high accuracy in experimental results. A clearance of 1.5 mm per side between the outer dimension of ties and steel formwork was allowed for mounting and insulating outer fiber strain gauges. Bending process was carried out such that a tolerance of ± 1mm was achieved against the specified dimensions. Steel bars used were mild steel hot rolled plain reinforcement which could be welded without causing any localized normalizing effects due to elevated temperatures.

To assure that the critical section (targeted test domain) for axial failure would occur around the center part of the column, ties were placed at lower spacing near the two ends of columns than specified values.

(3) Selection of concrete

Material uniformity is crucial for this experiments since member failure would be governed at the weakest section under axially uniform stress fields. As cover is eliminated, shrinkage must be essentially avoided, because it causes concrete to separate from ties and leave a gap resulting in premature failure. Bleeding and segregation should also be eliminated as far as possible to prevent any initial weak zones in top portions of castings.

Table 2 Mix proportion of self-compacting concrete

mixture kg/m^3	W	C	S	G	ad-mixture	slump flow
	185	520	850	899	2%	58cm

maximum size of aggregate : 20mm

In order to satisfy the above mentioned conditions, "self-compacting" high performance concrete[9] was utilized throughout the test program. All specimens were cast in a horizontal position to generate moulded loading ends, to promote better filling of restricted locations and to facilitate routing of strain gauge wires. Each specimen was cast with a single mix proportion, through a continuous operation as listed in **Table 2**.

(4) Instrumentation and testing

Axial mean strains were measured in the critical region of the column influential in the load carrying mechanism by π-type gauges mounted on cross rods integrally cast in columns. These rods were located symmetrically around the central ties at midway points containing one or two parallel pairs. Displacements between loading platens were also measured at the four corners of the columns by transformers as shown in **Fig.2**. This measurement merely serves to monitor the parallels of the platens during loading operation and as an cross check for axial strains.

Measurement of tie strains across and along tie arms using strain gauge pairs to obtain strain distribution that can be converted to stress distribution and spatial average stresses, is the most distinguishing aspect of this experiment. Continuous strain variation measurement as many strain gauge pairs is desired. In practice however, increase in the number of strain gauges results in increased area of voids between steel and concrete. Based on the above limitation, five pairs of strain gauges were applied per tie arm with careful treatment as shown in **Fig.3**.

Proper bedding between specimen ends and machine platens was achieved by applying a very rapid hardening cement grout layer placed between loading ends and machine platens. This bedding operation was performed in conjunction with adjustment for concentricity of loading. The loading rate of 3-5 μ/sec in axial strain was maintained from elasticity to non-linear zone of the specimen. Loading was generally continued beyond peak until at least the load carrying capacity was reduced to 80% of the maximum.

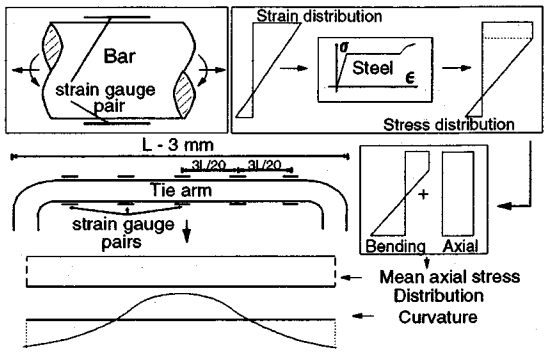

Fig.3 Spatial stress measurement in lateral r/f

(5) Experimental data processing

Concrete core is assumed to be bound by the centerline of ties. Though concrete cover over the ties was intentionally eliminated, a portion of concrete still remains invariably outside the center lines of ties (ie. between tie center lines and outside size). The thickness of this outside concrete portion depends on diameters of tie bar. Since this portion can not be categorized as core, its load carrying effect was assumed similar to unconfined concrete[3),6),11)-13)].

The load which is assumed to be carried by outer unconfined concrete is subtracted from the total load, to result in the load carried by the core and the core concrete stress.

Extreme fiber strains of steel ties were gathered and based on Kirchoff's "plane-section hypothesis", the strain distribution is obtained in a whole section. With the knowledge of steel stress-strain properties tested beforehand, the sectional fiber stress at each location is computed from strain reading. Here, the mean strain at a location is obtained by averaging the two strains of extreme fibers, while their difference divided by bar diameter results in the curvature. Since strain gauge locations were placed at equal intervals along tie arms and diameter of the ties is uniform, averaging of the mean stresses obtained at individual locations over the length of the tie arms results in steel stress averaged over its domain. Then using this average, spatial average confining stress of concrete core (σ_v) is obtained by Eq.(5). This value is of main point of this study.

Table 3 Effect of core size

Desig-nation	conf. cap. $1/2pf_y$ MPa	conf core peak (σ_v) MPa	conf. effect index by (α)	uncon-fined strength (f_{co}) MPa	core peak strength (f_{cc}) MPa	Strain at core peak (ε_{cc}) (micro)
P09-043 - small	7.13	6.38	0.90	38.0	53.0	10535
S25-119 - large	6.61	5.63	0.85	37.3	51.4	10386
T13-065 medium	7.22	6.56	0.91	36.7	51.8	10974

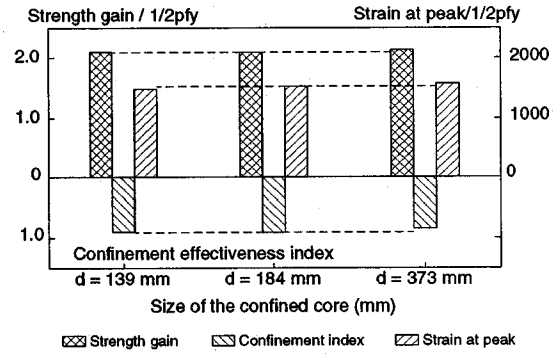

Fig. 4 Core size effect on confinement

4. CONFINEMENT EFFECTIVENESS OF LATERAL REINFORCEMENT

(1) Size of the concrete core

To purely verify the size effect on confinement effectiveness up to the ultimate capacity, other influencing factors on confinement were kept constant while changing the core size. For the purpose of this study, three specimens with outer sizes of 150, 200, and 400mm were utilized. The lateral reinforcement ratio (p=4%), spacing ratio (s/d =0.32), steel yield strength and unconfined concrete strength were kept nearly constant.

Specimens used for this comparison and results are compiled in **Table 3**. The experimental results of this series at the peak of the core are presented in the form of confinement effectiveness index, strength gain and strain at peak strength of core normalized by potential available confinement ($½pf_y$) in **Fig.4**. The above normalizing was done to account for the slight variations of potential available confinement. It is clearly seen from this figure that within the core sizes investigated, all three quantities remain virtually constant.

It can be concluded within this range that the size of the core does not have a significant influence on the confinement effect at the peak state. This conclusion is significant since, parametric studies can be conducted on small scale specimens to identify the bearing of other significant variables.

Table 4 Effect of r/f content and spacing

Desig-nation	conf. cap. $1/2pf_y$ MPa	conf core peak (σ_v) MPa	conf. effect index (α)	uncon-fined strength (f_{co}) MPa	core peak strength (f_{cc}) MPa	Strain at core peak (ε_{cc}) (micro)
C16-075	9.49	7.64	0.80	36.9	59.5	12655
D19-104	9.24	7.20	0.78	35.6	53.4	9449
O19x2-232	8.49	1.72	0.20	35.2	39.0	2734
A09-042	5.40	5.06	0.94	35.6	46.3	7187
H13-094	4.99	3.67	0.73	35.6	43.9	5371
I16-150	4.56	2.11	0.46	35.6	42.6	5660
J19-225	4.38	1.07	0.24	35.6	39.9	3642
M09-090	2.52	1.80	0.71	35.2	40.3	4439
N13-192	2.45	0.64	0.26	35.2	37.7	2330

(2) Reinforcement ratio and spacing

The amount of lateral reinforcement provided has been one of the major parameters adopted by previous studies. This quantity is here considered in terms of volumetric lateral reinforcement ratio. Secondly, the spacing of lateral reinforcement is addressed through the concept of dimensionless spacing ratio which depicts this parameter with reference to both core size and lateral reinforcement spacing. It was identified that the core size does not have a significant bearing on confinement effectiveness, when this normalized spacing ratio is used for representation of detailing of lateral reinforcement.

During these series of experiments, the point is to keep the maximum confinement (the potential of introducing confinement to core concrete by lateral steel : $½pf_y$) constant while varying the normalized spacing ratio. For all experiments, the same grade of steel was used with yield strength in a close range. Then, volumetric lateral reinforcement ratio becomes a direct indicator of potential confinement capacity in the succeeding discussions. Three reinforcement ratios referred to as high (p≈6%), medium (p≈3%) and low (p≈1.5%) were studied (See **Table 1**). The confinement and strength related results of this series are given in **Table 4**.

The axial mean stress and spatial average confining stress versus mean axial strain of concrete is plotted for medium reinforcement ratio (p≈3%) for different normalized spacing ratios in **Fig.5** through **Fig.8**. It can be seen from these figures that in all cases the developed confining stress with respect to axial loading is low at the beginning and increase afterwards. Initially, the lateral expansion is lower but, as the stress on the core increases, due to

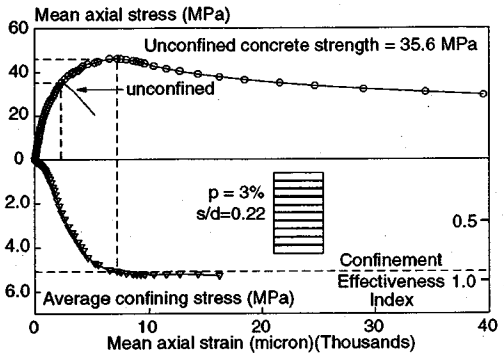

Fig.5 Stress-strain, confinement :s/d=0.22
-specimen A09-042 -

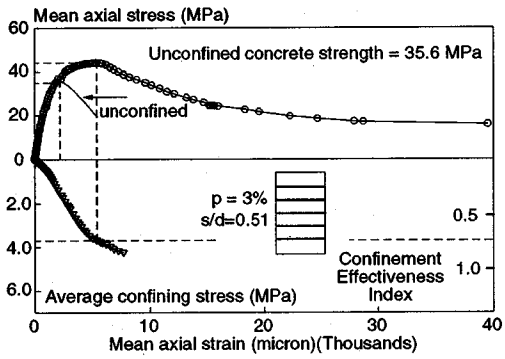

Fig.6 Stress-strain, confinement : s/d=0.51
- specimen H13-094 -

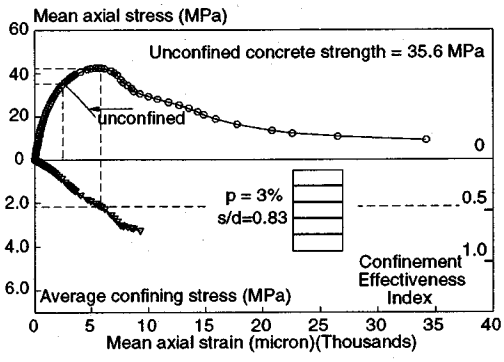

Fig.7 Stress-strain, confinement : s/d=0.83
- specimen I16-150 -

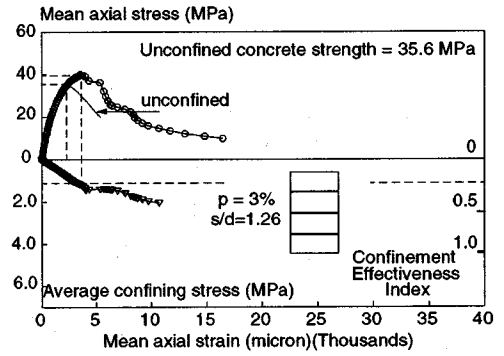

Fig.8 Stress-strain, confinement : s/d=1.26
- specimen J19-225 -

damage in the concrete volume, lateral expansion begins to increase at a higher rate.

However, in efficiently confined cores with smaller spacing developing high confining stresses closer to available capacity, the rate again gets less. This is due to the non-linearity generated in the confining steel caused by localized yielding coupled with the anisotropic non-linearity of core concrete. Since the behavior of confined concrete at the peak strength of the core is the prime interest in this study, the confinement developed at this level is addressed in detail through the followings.

Generated spatial average confining stress (σ_v) variation with normalized lateral reinforcement spacing ratio is given in **Fig.9** from which it can be seen that the increase in lateral reinforcement results in an increase of the absolute averaged confining stress. A clear reduction in the confinement action with the increase of the normalized spacing ratio is observed for all reinforcement ratios[5].

Variation of the confinement effectiveness index with the normalized spacing ratio for the different volumetric reinforcement ratios concerned are given in **Fig.10**. In the case of smaller spacing, almost all volume of lateral reinforcement yields (the index $\cong$1.0) but the larger spacing brings about partial yielding or entire elasticity of lateral ties (the index <0.6). This means that the experimental series listed in **Table 1** covers wider range of confinement effectiveness of lateral ties as shown in **Fig.10**. It is interesting to note that data for different reinforcement ratios indicates a mostly common path. Clearly, the general tendency of reduction of the confinement efficiency with the increase in spacing is confirmed.

These observations on induced confinement and the confinement effectiveness index can be rationally attributed to the effect of larger spacing which leaves a longer length of unsupported concrete between ties though theoretically the same maximum confinement potential is present. In this passively confined state, the stress developed in the confining agent depends on the ability of the confined concrete to transfer the stresses to the confining agent. Provision of wider spacing causes degradation in the uniformity of internal stress field resulting in higher local damage between ties[5]. This in turn culminates in the inability

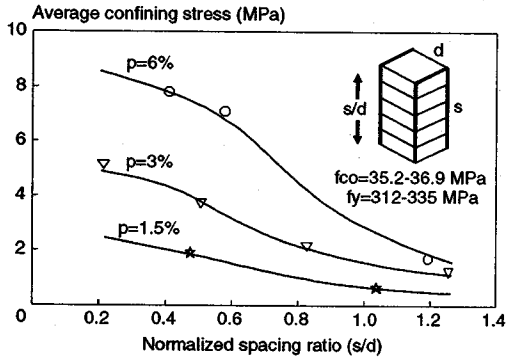

Fig.9 Average confinement at core peak

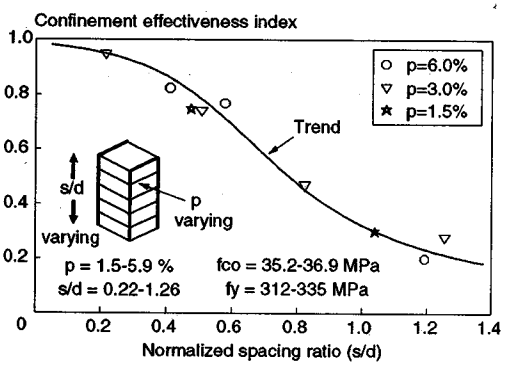

Fig.10 Confinement effectiveness index against spacing ratio

of concrete to develop higher magnitudes of confining stresses in steel.

(3) Flexural stiffness of lateral ties

If lateral ties act merely as truss agents, confining stress can only be induced from corners of ties to core concrete. Though this corner action will be predominant for smaller diameters of bars, larger size of bars associated with higher flexural and shear stiffness may induce further confinement through an entire interface between lateral ties and concrete.

This can be checked by experimentally obtained curvature of tie arms through strain measurements. Such measured curvature profiles in ties arms are shown for a pair of columns at their respective peak strengths in **Fig.11**. Columns compared has the same core and bar size but the spacing in the higher curvature developed column is half, while the reinforcement ratio is twice that of the companion. This indicates that with closer spaced confining arrangement the curvature induced in the bar is increased. Due to higher lateral restraint, greater lateral deformation of concrete, which is closely

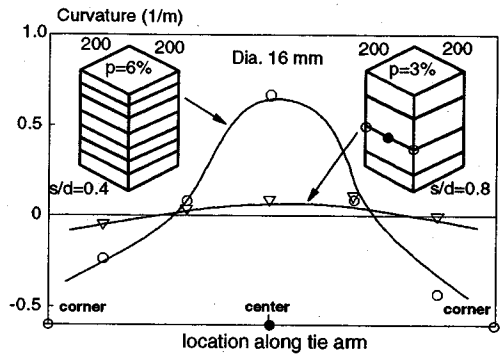

Fig.11 Curvature profiles of the same diameter tie (C16-075 and I16-150 in Table 1)

related to the curvature of lateral ties, is finally permitted.

These observations indicate different bending moments and shear forces in reinforcing bar sections. These induced moment has to be equilibrated with the contact forces acting on the core concrete. This contact force will enhance the confinement along tie arms in addition to corner action resulting from axial forces of bars between corners of the core. On this line, a special experiment was designed to remove forces transferred to concrete from steel with elimination of contact, except at the corner portions. This experiment was also intended to serve the purpose of verifying microscopic analysis.

Brudette and Hilsdorf conducted tests on this line by applying four steel angles tied by bolts to plain concrete square columns[1]. The contact between angles and column corners were filled with mortar. To reduce axial load being transferred to angles by friction, teflon strips had been used between angle and mortar strips. Reduction of stiffness of contact due to mortar strips and teflon layers, which leads to poor stress transfer across the corners, would have resulted in the scatter of the data observed. Due to this uncertain boundary condition, it is difficult to use this series of tests for verification of constitutive laws and FEM 3-D analysis.

For the purpose of this study, a different method was adopted. Ties were separated from core concrete by application of a deformable layer, except at corners to prevent transfer of contact forces. The length of the contact region at corners were decided based on the maximum size of coarse aggregate. The concrete outside centerlines of ties were eliminated by placing poly-styrene layers across tie spacing. Specifications of the special experiment are given in **Fig.12**. The thickness of the deformable layer was kept low to minimize the effect of

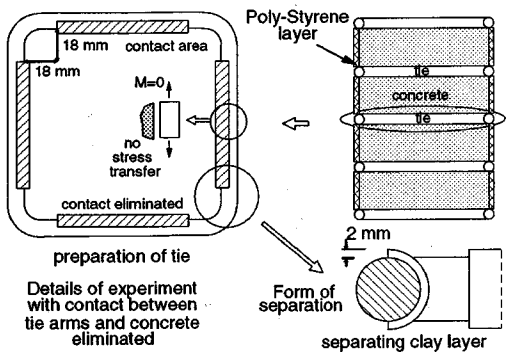

Fig.12 Specifications for corner action test

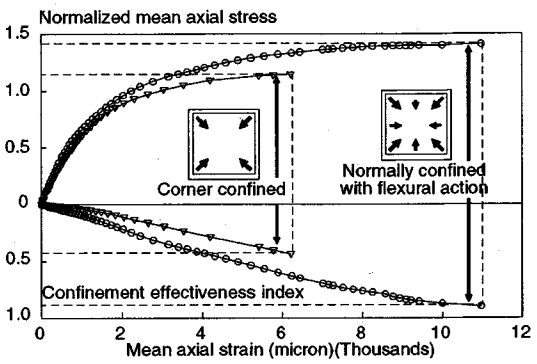

Fig.13 Stress-strain, confinement for corner and contact actions

Table 5 Effect of flexural stiffness of lateral bars

	limit conf. 1/2pfy	conf. peak by σ_v	eff. index by α	uncon-fined strength	peak strength	peak strain
T13-065 beam eff.	7.22 MPa	6.56 MPa	0.91	36.7 MPa	51.8 MPa	10974 micro
U13-65-C corner eff.	7.22 MPa	3.15 MPa	0.44	35.8 MPa	41.1 MPa	6205 micro

reduction of core area. Observed curvature at the tie center was nearly zero in the ascending portion of stress-strain diagram. But, it must be reported that some contact took place after the peak due to geometrically larger dilatancy of core concrete.

To make a comparison with the above mentioned experiment, a control specimen was used with equal lateral reinforcement ratio, spacing ratio, core size, tie size and strength of reinforcement. In this specimen contact between concrete and lateral reinforcement was maintained at all locations. Nearly the same unconfined concrete strength was attained. Results of the two tests are given in **Table 5**.

In both cases the maximum available confinement capacity is the same, but it is clearly seen from **Fig.13** that the corner confined column has developed considerably less confinement stress at the core peak compared to normally confined concrete. Mean axial stress normalized by unconfined concrete strength and confinement effectiveness index plotted against mean axial strain in this figure indicates a definite loss in the peak axial strength of the core. The axial strain at peak strength is seen to be reduced too by more than 40% due to absence of contact action. Further, the developed confinement is about 50% of the equivalent normally confined column.

It can be concluded that the flexural stiffness and contact contribution of tie arms play some substantial role in the enhancement of confinement effectiveness. This factor may not be significant in cases of confinement with lower stiffness ties, under low reinforcement ratios. However, it becomes specially significant in the cases of higher reinforcement ratios with larger diameter bars as compared to core size. In analytical studies on confinement including micro-mechanical model based FEM studies, beam action as well as corner action should be accounted.

5. ENHANCED CAPACITY BY LATERAL REINFORCEMENT

In this study emphasis is placed on the enhancement of peak strength of the concrete core. This aspect is significant since it indicates the structural reliability and soundness. Furthermore, in the engineering point of view, the maximum load carrying capacity of a concrete column is of much importance for members subjected to higher axial forces and combined bending. Also, the axial strain at the peak strength is addressed.

(1) Capacity gain and reinforcement ratio

It had been assumed in some previous researches that the strength gain by lateral reinforcement is proportional to the product of reinforcement ratio and steel yield strength[11),13)]. It is interesting to note that half the above product represents the potential maximum confinement denoted by $\frac{1}{2}pf_y$. This assumption may be approximately correct for closely placed lateral reinforcement in the case of circular columns[4)]. For square columns, validity of this assumption has to be verified since this condition is only realized when all provided steel assumes yield at the peak strength of the core. As a matter of fact, 3-D FEM analysis of square columns subjected to axial compression reported that elasticity of steel lateral ties remains even when the axial concrete capacity is performed[4)].

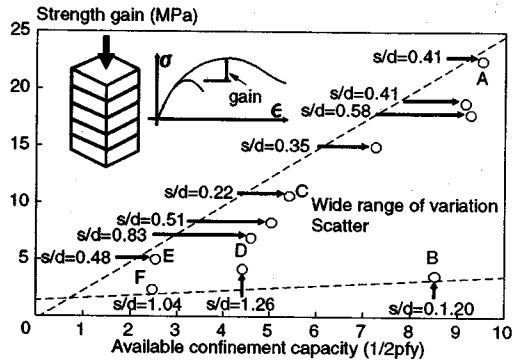

Fig.14 Strength gain and potential confining capacity at peak strength of core

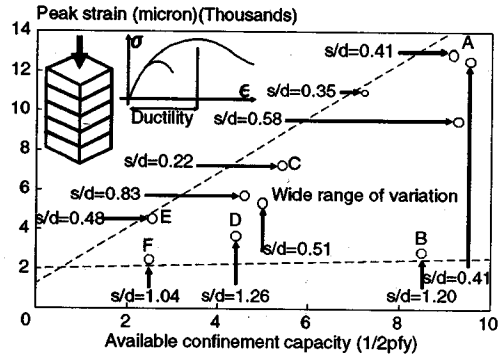

Fig.15 Ductility and potential confining capacity at the peak strength of core

In order to check whether this assumption is correct, the strength gains of the experimental ranges were plotted against the maximum available confinement in **Fig.14**. Since the steel strengths used for the study are in a close range, discussion on the figure is done on reinforcement ratio basis. This figure shows a considerably high overall scatter. For lower reinforcement ratios, the scatter is about 50% of the higher strength specimen as points marked *E* and *F* are compared. As the reinforcement ratio increases a very prominent scatter is developed. This is confirmed by observation of the points *C* and *D* for medium reinforcement ratio, while points *A* and *B* for high reinforcement ratio show the widest scatter. From the spacing ratios indicated at each data point a clear trend of higher strength gains for lower spacing at a given reinforcement ratio is observed. The axial strain at the peak strength also exhibits a very similar scatter, as seen from **Fig.15** depicting peak strain against the maximum available confinement capacity.

From the above discussion it is very clear that there exists no direct relation between the volume of

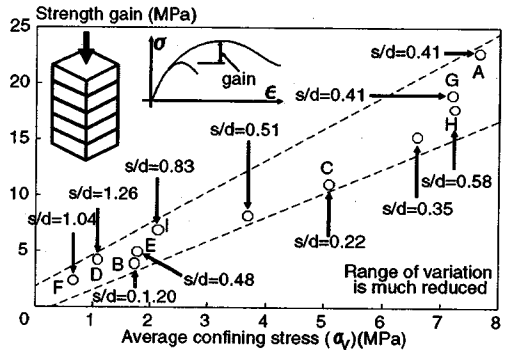

Fig.16 Strength gain with induced average confining stress at the peak of the core

steel provided and the strength gain, or ductility for square columns. The above observations indicate a strong influence of spacing of ties which had been pointed out. Then, strength enhancement has to be studied under two main parameters of the amount of reinforcement and the spacing of this discrete reinforcement.

(2) Actually induced confinement by steel

Spatial average confining stress by steel which is the actually induced confinement and found to be dependent on the spacing of lateral ties, should be a better parameter to be related with strength enhancement. To examine this possible relation **Fig.16** is composed with strength gain against the actually induced confining stress at peak strength of core for different reinforcement and spacing ratios. It is seen from comparison of data points discussed in **Fig.14** that a better relation and a tendency with less scatter is generated. The point *B* which was nearly under point *A* in **Fig.14** has moved quite close to the origin in **Fig.16**. also the point *D* in **Fig.14** which was close to point *C* has moved closer to the origin. The same can be said for points *E* and *F*. The shifting of these points indicates that the relation between the new parameter (ie. the actually induced average confinement) is a better representation to be related with the strength gain. In a rational view point the actually induced confinement should be related with the strength enhancement due to confinement.

Fig.17 relates the axial strain at the peak strength with the induced confinement. In this figure the relative variations of points *A-B*, *C-D* and *E-F* shows similar trends observed in the strength gain comparison. Since the confinement effectiveness index is related directly with the induced averaged confinement, this index would become a good

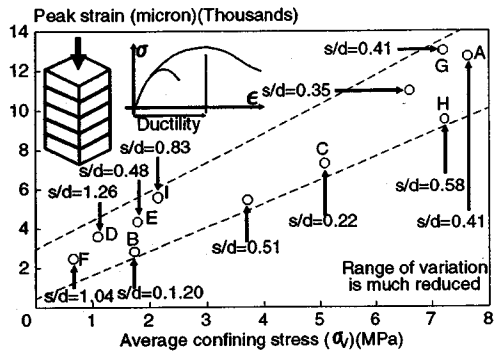

Fig.17 Peak strain with induced average confining stress at the peak strength of the core

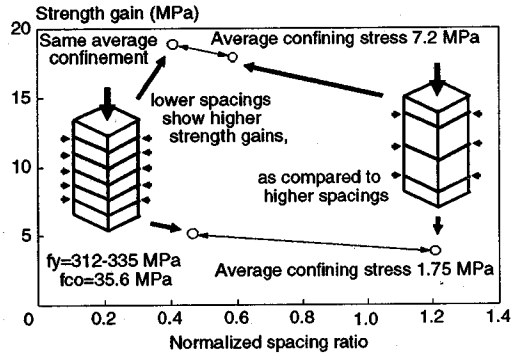

Fig.18 Strength gain under same average confining stress

representation of the strength enhancement efficiency due to confinement. In rational design formula, this index should be evaluated either empirically or analytically, but few research provides the actually induced confinement from steel to core concrete. Thus, an analytical approach which is systematically checked in use of verification data will be powerful for formulating the confinement effectiveness index of general cases.

Nevertheless, still a lower but, significant scatter is apparent in the data, which could be attributable to experimental scatter. However, it is seen that when two sets of data *E,B* and *G,H* in **Fig.16** are considered, each pair has nearly the same induced confinement whereas the strength gains are not equal. This effect is much more pronounced when the same two pairs of points are compared in **Fig.17**. It is very clear from the two figures that, points *E* and *G* as compared to points *B* and *H* shows higher strength gain as well as ductility. This observation tends to suggest that, a further influencing factor could be prevalent, which had not been accounted.

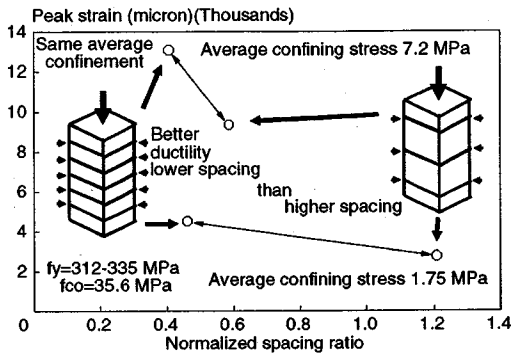

Fig.19 Peak strain under the same average confining stress

(3) Double effect of spacing to core size ratio

In the above discussion it was observed that two sets of results with nearly same induced spatial average confining stress, developed different strength gain and ductility.

When the detailing parameters of the two pair of specimens were checked, it was realized that the higher strength gain or ductility were developed by the specimens with lower spacing than the companions. This suggests that the spacing has a second effect on the strength enhancement due to confinement. The observation is presented in **Fig.18** for strength gain and in **Fig.19** for peak ductility comparisons under these conditions.

Since sectional confining stress varies along the axis of the column, though the volumetric average stress is the same, variation for higher spaced column will be more than the lower spaced counterpart. It can be rationally assumed that the confining stresses at the least confined section (ie. midway between the ties), govern the peak strength and corresponding ductility. Based on this assumption, the wider spaced column should develop lesser strength gain and ductility as compared to the close spaced specimen even though the same volumetric confining stress is induced to concrete core.

This finding is quite significant since it directly implies that, the spacing of lateral ties has double effects on enhancement of capacity due to confinement. In previous studies, these dual effect has not been observed since the induced confinement had not been comprehensively measured. Through the extensive strain measurements on ties which enabled the average confining stress to be computed, this discovery was made possible.

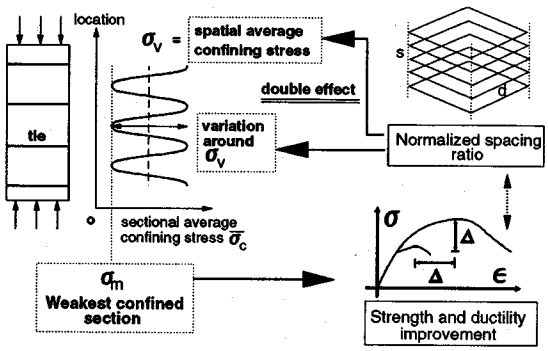

Fig.20 Double effect of r/f spacing

First effect of spacing is applied when the induced average confining stress is considered where, the ability of steel to resist the expansion of concrete is supplemented when spacing becomes lesser. This in turn results in the expanding concrete inducing higher stresses in the steel domain. Such induced stresses in steel are transferred back to concrete in the form of confinement spread over the concrete volume.

The second effect is applied in the determination of the weakest confined section depending on the distribution of such induced confinement along the column axis. Since the lowest confined condition should govern the strength enhancement of the member, wider spaced detailing should result in a lower level as compared to closely spaced case even though the actual induced confinement stress is performed. The influence of the main parameters on confinement is depicted in **Fig.20**. Analytical method based on micro mechanical models can be used as another method to verify the above discussed argument.

6. CONCLUSIONS

Experimental observations conducted under theoretical conceptual background provided a valuable insight into the phenomenon of passive lateral confinement by steel ties on square columns under axial compressive loading. Through this study, mechanically defined spatial average confining stress was measured for the first time for square lateral reinforcement. Confinement effectiveness index with mechanical basis was newly introduced as the ratio of above quantity to the potentially available confinement capacity of the lateral reinforcement.

Lateral steel does not always come to yield at the peak strength of a square confined core as assumed in many previous studies. This was experimentally identified through spatial strain measurement in lateral ties converted to stress distribution. Therefore, actually developed confinement does not reach the maximum potential confinement capacity of lateral reinforcement, indicating that there is no direct relation between the potential confinement capacity and the enhancement in strength of a confined core.

The actually developed spatial average confining stress was found to be the basic governing quantity related to the confinement effectiveness as well as strength enhancement due to confinement. Through the experimental program, amount of the lateral reinforcement given in terms of volumetric lateral reinforcement ratio and tie spacing expressed as the spacing to core dimension ratio were found to be the most influential on the induced spatial average confining stress. Secondly, the flexural contribution of lateral tie arms depending on the diameter and span of each arm and contact action was found to have a significant beneficial effect on the confinement action. Therefore, this effect should not be neglected in analytical formulations on confinement effectiveness.

Strength gain of confined core was identified to be influenced by the developed average confining stress and the spacing of the ties governing lateral confining stress uniformity. Since developed average confining stress is also dependent on the tie spacing, it was found to have double effects on the strength enhancement due to confinement.

The core size was found to have no appreciable effect on the confinement effectiveness of lateral ties in the range examined (core size range 139 mm -373 mm).

ACKNOWLEDGMENT: The authors express their gratitude to Prof. Okamura, the University of Tokyo for his guidance. This study was financially supported by Grant-in-Aid for scientific research No.05452226 from The Ministry of Education of The Japanese Government in 1994.

REFERENCES

1) Brudette, E. G., and Hilsdorf, H. K.: Behavior of Laterally Reinforced Concrete Columns, *Journal of the Structural Division*, ASCE, Vol. 97, pp. 587-602, 1971.

2) Carreira, D. J., and Chu, K. H.: Stress-Strain Relationship for Plain Concrete in Compression, *American Concrete Institute Journal*, Vol. 82, pp. 797-804, 1985.

3) Gangadharam, D., Nagi Reddy, K.: Effect of Cover Upon the Stress-Strain Properties of Concrete Confined in Steel

Binders, *Magazine of Concrete Research*, Vol. 32, pp. 147-155, 1980.

4) Irawan, P. and Maekawa, K.: Strength and Damage Analysis of Concrete Confined by Steel Casing, *Journal of Materials, Concrete Structures and Pavements*, JSCE, Vol.20, No.472, pp.97-106, 1993.

5) Irawan, P. and Maekawa, K.: Three-Dimensional Analysis on Strength and Deformation of Concrete Confined by Lateral Reinforcement, *Journal of Materials, Concrete Structures and Pavements*, JSCE, Vol.20, No.472, pp.107-118, 1993.

6) Karsan, I. D., and Jirsa, J. O.: Behavior of Concrete Under Compressive Loadings, *Journal of the Structural Division*, ASCE, Vol. 95, pp.2543-2563, 1969.

7) Maekawa, K., Takemura, J. Irawan, P., and Irie, M.: Triaxial Elasto-Plastic and Continuum Fracture Model for Concrete, *Concrete Library*, JSCE, No. 22, pp. 131-161, 1993.

8) Okamura, H., and Maekawa, K.: *Nonlinear Analysis and Constitutive Models of Reinforced Concrete*, Gihodo-Syuppan, Tokyo, 1991.

9) Okamura, H., Maekawa, K., and Ozawa, K.: *High Performance Concrete*, Gihodo-Syuppan, Tokyo, 1993. (in Japanese).

10) Sargin, M.: Stress-Strain Relationships for Concrete and Analysis of Structural Concrete Sections, *Study No. 4*, Solid Mechanics Division, University of Waterloo, Waterloo, Ontario, Canada, 1971.

11) Scott, B. D., Park, R., and Priestley, M. J. N.: Stress-Strain Behavior of Concrete Confined by Overlapping Hoops at Low and High Strain Rates, *ACI Journal Proceedings*, Vol. 79, pp. 13-27, 1982.

12) Sheikh, S. A., and Uzumeri, S. M.: Strength and Ductility of Tied Concrete Columns, *Proceedings*, ASCE, Vol. 106, pp. 1079-1102, 1980.

13) Somes, N. F.: Compression Tests on Hoop Reinforced Concrete, *Proceedings*, ASCE, Vol. 96, pp. 1495-1509, 1970.

(Received November 25, 1994)

コアコンクリートの拘束に対する横補強筋の有効性

Tirath Manoja PALLEWATTA, Paulus IRAWAN and Koichi MAEKAWA

本研究は横方向に補強されたコンクリートの挙動について，実験的手法により論ずるものである．研究の主たる目的は，横補強鉄筋による拘束効果を力学的に妥当な形で定量化すること，及び非線形３次元コンクリート構成則を柱部材中に発生する実拘束応力下で検証するに相応しい，信頼性の高いデータを得ることである．そこで，完全併合型の横補強筋を採用し，かぶりを省き，均一なコンクリートを形成するために自己充填コンクリートを用いた．コアコンクリートに対する横補強筋の拘束効果に関する影響因子を抽出し，もって耐荷力予測式等の巨視的モデル化を開発，かつ検証するための基礎情報を得た．横拘束鉄筋に発生する応力を詳細に計測・分析することより，コアコンクリートに導入される３次元平均拘束応力を定量的に示した．